Analysis of Non-Linear

Rainfall-Runoff Process

Willi H. Hager

École Polytechnique Fédérale de Lausanne,
CH-1015, Switzerland

Rainfall runoff phenomena in small watersheds are favorably modelled using the kinematic wave approach. The present investigation considers excess rainfall as time dependent but ignores spatial effects. Solutions of a recent approach are analyzed for a complete cascade consisting of catchment area and small stream. Typical cases are discussed and results include predictions of maximum discharge at the watershed outlet, corresponding time to peak and the overall description of the resulting hydrograph. Criteria concerning the applicability of the kinematic wave approach are given, and examples illustrate the computational procedure.

Introduction

Kinematic wave theory is a simple method to describe unsteady flow in open channels. Compared to the full one-dimensional flow equations, a modification of the dynamical properties leads to a single equation for either flow depth or discharge as a function of time and space. This approach is particularly well suited for flows over small watersheds (Raudkivi 1979). During the last two decades a number of hydrological models have been proposed, some of which are summarized by Eagleson (1970). The simplest of these considers excess precipitation as independent of time and space (Wooding 1965 and 1966).

Recently, a simple hydrological rainfall runoff model has been developed for a single-peaked excess rainfall (Hager 1984a). Solutions have been represented

graphically, and it is possible to consider a cascade by using the plots repeatedly. The major advantage of such a model is its *elementary* application to realistic runoff processes in small basins under relatively high excess precipitation. Its disadvantage is a semi-analytical adapting process, by which input data for a following cascade must be computed.

The present investigation reconsiders in more detail the aforementioned solutions. Effects of the catchment area shape, the roughness coefficient and the bottom slopes of both catchment area and small stream on the resulting hydrograph at the basin outlet will be studied. The computational procedure is explained in detail and conclusions include recommendations, which might be useful for more sophisticated, hydrological rainfall runoff models.

Governing Equations

Unsteady flows with predominate flow direction may be modelled using the de Saint-Venant equations, which balance mass and longitudinal momentum (Eagleson 1970). Overland and small stream runoff is characterized by two distinct properties

i) flow depth is much smaller than the elevation difference of two typical points of the reach,

ii) typical Froude number is smaller than unity.

These peculiarities allow simplification of the original equations (Raudkivi 1979); the resulting system

$$\frac{\partial h}{\partial t} + \frac{\partial q}{\partial x} = p \tag{1}$$

$$S_0 = S_f \tag{2}$$

corresponds to the *kinematic wave approach* described extensively by Lighthill and Whitham (1955). Eq. (1) is the full continuity equation with h flow depth, t time, q discharge per unit width, x longitudinal coordinate, p lateral inflow or outflow. Eq. (2) is the simplified dynamical relation with S_o bottom slope and S_f frictional slope, respectively. For turbulent flow S_f may be expressed by the Manning-Strickler formula

$$S_f \equiv \frac{q^2}{K^2 \, h^{10/3}} \tag{3}$$

in which $K = 1/n$ is the friction coefficient. It may be shown (Hager 1984b) that both K and S_o can be approximated by appropriate *averages* along the considered reaches. For *small watersheds* it is further reasonable to assume excess rainfall only as a function of time, $p = p(t)$, thereby neglecting spatial effects. A typical time

distribution of the excess precipitation provides the relation (Hager 1984a).

$$p(t) = p*(Te^{1-T})^m \qquad (4)$$

in which p^* is the maximum excess precipitation at time $t = t^*$; $T = t/t^*$ is non-dimensional time with $T = 0$ as start of excess precipitation, and m is the hydrograph shape parameter.

Ensuing considerations are restricted to *heavy precipitations,* implying an initially dry catchment area. For relatively *long* catchment areas and streams the inflow depths at their respective highest point are much smaller than a typical flow depth (Hager and Hager 1985). Asymptotically, the flow depths $h(x_i = 0,t) = 0$ in which index i referes to either side of the catchment area and to the small stream at their bisecting line. Eqs. (1) and (2) then must be solved using the conditions $q(0,t) = q(x,0) = 0$. The scalings

$$T = \frac{t}{t*} \quad , \quad X = \frac{x}{KS_0^{1/2} \, p*^{2/3} \, t*^{5/3}}$$

$$Y = \frac{h}{p*t*} \quad , \quad Q = \frac{q}{KS_0^{1/2} \, p*^{5/3} \, t*^{5/3}} \qquad (5)$$

transform Eqs. (1) and (2) into (Hager 1984a)

$$\frac{\partial Y}{\partial T} + \frac{5}{3} Y^{2/3} \frac{\partial Y}{\partial X} \equiv (Te^{1-T})^m \qquad (6)$$

$$Q \equiv Y^{5/3} \qquad (7)$$

subject to the conditions $Q(X = 0) = Q(T = 0) = 0$. This has been solved using the method of characteristics (Hager 1984a). Fig. 1 shows hydrographs $Q(T)$ for various significant locations X. There are three domains to be distinguished from each other

i) *increasing discharge:* for $X \rightarrow \infty$ hydrographs are given by the *S*-shaped "steady state" solution,
ii) *maximum discharge:* for finite values of X, hydrographs separate from the first curve to attain the maximum discharge $Q_{max}(X)$ and corresponding time is $T_{max} = t_{max}/t^*$,
iii) *receding discharge:* for $T > T_{max}$, discharge is decreasing to reach asymptotically $Q = 0$.

Once the basic parameters p^*, m, t^*, K, S_0 are prescribed, Fig. 1 allows a direct and simple evaluation of the governing hydrograph at any location of the catchment area. Based on these results the runoff behaviour of the small stream may be investigated. This is achieved by accounting for the stream parameters K, S_0 and
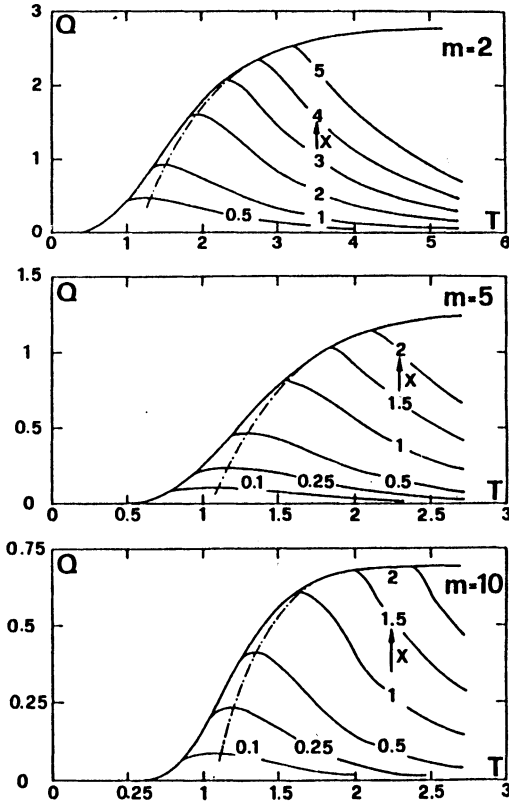
293

Willi H. Hager

Fig. 1.
Non-dimensional hydrographs $Q(T)$ for various locations X and precipitation shape factors $m \equiv 2$ (top), $m \equiv 5$ (center), $m \equiv 10$ (bottom); the dotted dashed curve indicates the locations of Q_{max}.

proper values for p^*, m, t^* regarding the transition from catchment area to small stream. Finally, one may use the results for a *cascade model,* thereby having in mind the approximate and simplified description of the rainfall-runoff model. An extensive discussion of the computational procedure and illustrative examples are given in Hager (1984a).

Maximum Lateral Inflow

The *maxima* of the lateral inflow to the stream are indicated in Fig. 1 by the dotted-dashed curves. According to Hager (1984a)

$$Q_{max} = X , \qquad X << 1 \tag{8}$$

By introducing the new scalings

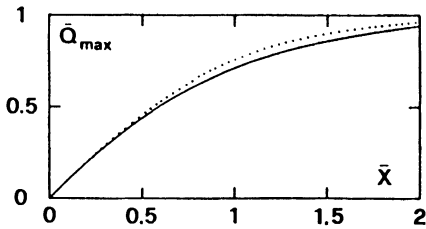$$\bar{X} = \frac{X}{Q_{abs}} , \qquad \bar{Q}_{max} = \frac{Q_{max}}{Q_{abs}} \tag{9}$$

294

Fig. 2. Relative maximum discharge $\bar{Q}_{max}$ as function of relative distance $\bar{X}$ according to Fig. 1 (solid curve, for all m) and Eq. (11) (dotted curve).

in which $Q_{abs} = Q_{abs}(m)$ is maximum possible discharge, Eq. (8) may be generalised. An approximation for Q_{abs} is (Sinninger and Hager 1984)

$$Q_{abs} = (e \times m^{-0.54})^{5/3} \qquad (10)$$

in which e is Euler's number. For $m = 2, 5, 10$ the respective values of Q_{abs} are exactly 2.780, 1.244, 0.688, compared to 2.837, 1.244, 0.677 from Eq. (10).

Fig. 2 shows a plot of $\bar{Q}_{max}(\bar{X})$ for $m = 2, 5, 10$ according to Fig. 1. It is noted that all curves become identical, following Eq. (8) for small $\bar{X}$ but tending to unity for large $\bar{X}$. The approximation

$$\bar{Q}_{max} = Tanh(\bar{X}) \qquad (11)$$

is also plotted as dotted curve. Deviations between the two are less than 5%.

Time to Peak and Hydrograph Shape

The solutions $Q(T)$ according to Fig. 1 have more or less the shape of the excess precipitation distribution, Eq. (4). A hydrological cascade thus may approximately be achieved by considering the transition from overland to stream flow as governed by the aforementioned relation, thereby modifying the respective scalings. Evidently, the peak discharge Q_{max} will be fixed, such that time to peak, t_{max}, must be adapted in order to fit best with the exact solution. Fig. 3 shows i) the exact solution $Q(T)$ for $X = 2$ and $m = 10$ according to Fig. 1, ii) the curve

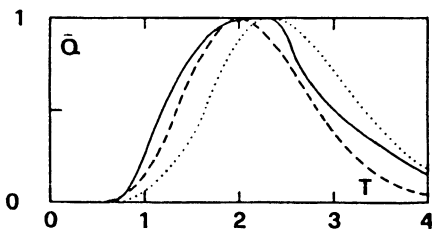$$\bar{Q} = [\bar{T} \exp(1-\bar{T})]^{10} \qquad (12)$$

Fig. 3. Explanation of the effect of adapted T_{max} for fixed maximum discharge: hydrograph according to Fig. 1 (solid curve) is badly reproduced by setting $T_{max,adp} = T_{max,eff}$ (dotted curve) but fits better if $T_{max,adp} < T_{max,eff}$ (dashed curve).
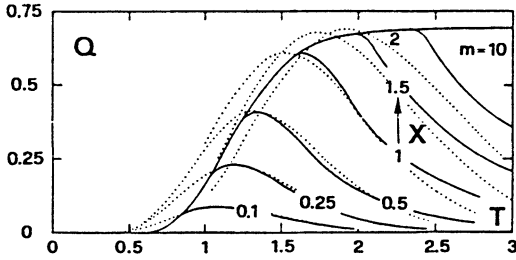
295

Fig. 4.
Comparison of hydrographs $Q(X,T)$ according to Fig. 1 (solid lines) and hydrographs according to Eq. (12) for $m \equiv 10$.

in which $\bar{T} = T/T_{max} = t/t_{max}$ with t_{max} as time to peak according to Fig. 1 and iii) Eq. (12) with an adapted value for t_{max}, namely

$$T_{max} \equiv 1.1 + 0.4 X, \quad X > 0 \tag{13}$$

in which $T_{max} = t_{max}/t^*$. It is seen from the figure (and may be shown for all other X) that the latter approach, accounting for Eq. (13), leads to a reasonable agreement with the exact solution.

Fig. 4 compares $Q(T)$ according to Fig. 1 with the adapted curves using relations Eq. (11) for $\bar{Q}_{max}$ and Eq. (13) for T_{max} and the discharge distribution Eq. (12) for $m = 10$. Deviations between two corresponding hydrographs are sufficiently small in a wide range of T and X. Note that Eq. (12) is valid for all m shown in Fig. 1; it may be regarded as approximate solution of Eqs. (6) and (7).

Computational Aspects

The original method proposed by the author (1984a) consisted in a semi-graphical approach. After every cascade hydrographs had to be approximated by a relation analogous to Eq. (4), thereby specifying parameter t^*, p^* and m for the subsequent cascade.

The above approach suggests that the precipitation distribution $p = p(t,t^*,m)$ should be approximated with Eq. (4) by setting $m = 10$ and adapt t^* such that the resulting hyetograph fits best with the effective excess rainfall distribution (see also latter example).

Let indices "1" and "2" refer to properties of the catchment area and to the small stream, respectively, and "i" to either of the two cascades, Then, from Eq. (10), $Q_{abs}(m = 10) = 0.69$, whence

$$Q_{max,i} \equiv 0.69 \; Tanh\left(\frac{X_i}{0.69}\right), \quad m = 10 \tag{14}$$

from Eq. (11) for cascade i. Time to peak, $T_{max,i}$, for X_i is then given by Eq. (13), and the complete hydrograph is prescribed by Eq. (12).

Discussion of Particular Cases

The cascades "catchment area-small stream" of which the non-dimensional lengths X_i are either very small or large may be treated by a simple approach.

i) Case X≪1

For small (positive) X, or $\bar{X}$ according to Eq. (9), relation Eq. (11) simplifies to $Q_{max} \equiv X$. With X according to Eq. (5)$_2$,

$$q_{max,1} = p_1^* x_1 \tag{15}$$

whence, with $p_2^* = q_{max,1}/b_1$

$$q_{max,2} \equiv \frac{p_1^* x_1 x_2}{b_1} \tag{16}$$

or, for the maximum discharge in a small stream of total width B

$$\widetilde{Q}_{max,s} = p_1^* x_1 x_2 \frac{B}{b_1} \tag{17}$$

This simple result states that the maximum discharge $\bar{Q}$ in (m³/s) at the watershed outlet with sides $x_1(B/b_1)$ and x_2 is equal to the maximum excess precipitation p_1^* times the surface $A = x_1 x_2 B/b_1$ (note that B refers to the complete stream width while b_1 corresponds only to the stream width relating to the considered side of the catchment area).

Eq. (17) holds for both *time dependent excess rainfall* and *steady flow conditions* with $p_1 = p^* = $ constant. Surprisingly enough Eq. (17) contains neither K_i nor $S_{0,i}$ of the catchment area and the small stream. Consequently the geometrical shape of the basin and the flow parameters have no effect on the maximum discharge.

Before investigating the necessary conditions in order that $X_i \ll 1$, let us compute time to peak of the hydrograph at the watershed outlet. Using twice Eq. (13) yields

$$t_{max,s} \equiv t_1^* (1.1 + 0.4 X_1)(1.1 + 0.4 X_2) \tag{18}$$

or, when inserting values of X_2

$$t_{max,s} = t_1^* (1.1 + 0.4 X_1)\left(1.1 + \frac{x_2}{K_2 S_{0,2}^{1/2} \left(\frac{p_1^* x_1}{b_1}\right)^{2/3} t_1^{*5/3}(1.1 + 0.4 X_1)^{5/3}}\right) \tag{19}$$

This may equally be written as

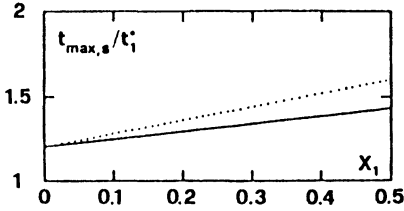$$t_{max,s} = t_1^* (1.1 + 0.4 X_1)\left(1.1 + \frac{X_1 X}{(1.1 + 0.4 X_1)^{5/3}}\right) \tag{20}$$

297

Fig. 5. Evaluation of Eq. (20) for $\chi \simeq 0$ (solid curve) and $\chi \equiv 1$ (dotted curve).

Fig. 5 is a graphical evaluation of Eq. (20) in which

$$\chi \equiv \frac{x_2}{x_1} \left(\frac{b_1}{x_1} \right)^{2/3} \left(\frac{K_1 S_{0,1}^{1/2}}{K_2 S_{0,2}^{1/2}} \right) \tag{21}$$

Usual orders of $K_1/K_2 \simeq 1/2$ and $(S_{0,1}/S_{0,2})^{1/2} \simeq 2$; consequently the two last terms of Eq. (21) compensate approximately. Since $(b_1/x_1) \ll 1$ and $(x_2/x_1) = 0(1)$, thus $\chi \ll 1$, one may set

$$t_{max,s} \cong 1.1 \, t_1^* (1 : 1 + 0.4 X_1) \quad , \quad X_i \ll 1 \tag{22}$$

The determination of the hydrograph at the watershed outlet is now simple and straightforward. With

$$\hat{T} \equiv \frac{t}{t_{max,s}} \quad , \quad \hat{Q} = \frac{\tilde{Q}}{\tilde{Q}_{max,s}} \tag{23}$$

in which $t_{max,s}$ and $\tilde{Q}_{max,s}$ are given by Eqs. (22) and (17), respectively,

$$\hat{Q}(\hat{T}) = [\hat{T} \exp(1-\hat{T})]^{10} \tag{24}$$

Example

Consider a catchment area with a small stream of $B = 3$ m width, $K_s = 18 \text{ m}^{1/3}\text{s}^{-1}$, $S_{0,s} = 0.018$. The catchment area may be simplified as two rectangular planes having widths 850 m and 250 m, respectively, (thus $b_1 = 3 \times 850/ (1,100) = 2.3$ m) and $S_{0,c} = 0.08$, $K_c = 8 \text{ m}^{1/3}\text{s}^{-1}$. The length of the stream is $x_s = 3,450$ m (see also Hager 1984a).

At time $t = 0$ rainfall starts with characteristical parameters $p^* = 2.5$ mm/h (excess rainfall), $t^* \equiv 6$ h and $m \equiv 5$. Since the present investigation considers only hydrograph shape parameters $m = 10$, one has to choose for $t^* = 8$ h (start of rainfall two hours earlier as indicated above, see also later Fig. 6), $p^* = 2.7$ mm/h and $m = 10$ (excess rainfall volumes are almost identical for the two of the representations). What is the resulting hydrograph at the basin outlet?
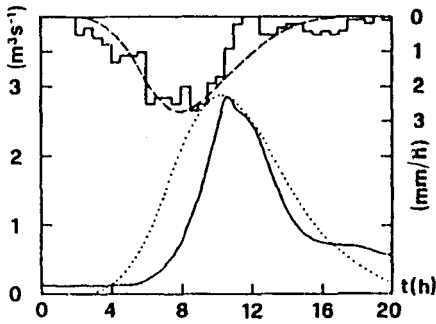
298

Fig. 6.

Comparison between present simplified formulation and observations (Jaton 1982); excess hyetograph (above) at half-hours intervals and adapted excess hyetograph (dashed curve); resulting hydrographs (below) at basin outlet (dotted curve computed).

With $X_1 = X_c = 0.168$ and $X_2 = X_s = 0.0106$ the condition $X_i \ll 1$ is fulfilled. According to Eq. (17) maximum discharge for the watershed is $\bar{Q}_{max,s} = 0.0027 \times 1{,}100 \times 3{,}450/3{,}600 = 2.87$ m^{3}s^{-1}. According to Eq. (22), corresponding time to peak obtains $t_{max,s} = 1.28\ t_i^* = 10.24$ h. Fig. 6 compares observations described by Jaton (1982) and discussed by Hager (1984a) with the present formulation, and a fair agreement between the two is noted.

Computed discharge at $t < t_{max,s}$ is overestimated; this fact must be attributed to the adapting process performed in Fig. 4. Given the simplicity of the present approach, the result must be regarded as a fair estimate of the effective runoff process.

The condition to be fulfilled in case i) is that X_i (whence both X_c and X_s) must be small when compared to unity. Since K_i are more or less fixed ($5 < K_i < 25$), and the effect of the bottom slopes may be regarded as subordinate $X_i \propto 1/S_{0,i}^{1/2}$, X_i becomes *small* for

- relatively small catchment areas (say surface smaller than 10 km^2),
- heavy maximum excess precipitation p_1^* (say more than 2 mm/h),
- long time to peak t_i^* (say more than 5 hours).

Whenever all of these conditions are fulfilled, case i) may be applied. Evidently, it will be advisable to check both of the parameters, X_c and X_s, to be smaller than unity. An upper limit of X_i for which case i) applies is, roughly, $X_i < 0.30$ (see Fig. 2).

Appendix I gives further information about the basic requirements regarding the kinematic wave theory. It is found that

- the product $(K_i\sqrt{S_{0,i}})$ must be smaller than 3 for both, catchment area *and* small stream in order that dynamical wave effects are insignificant, and
- the ratio $h_{max,i}/(S_{0,i}x_i)$ be much smaller than unity (say < 0.05) in order that diffusive effects remain insignificant. According to (Hager and Hager 1985) this latter condition may also be expressed as $p_{max,i} < 0.07\ g^2/(K^3\sqrt{S_0})_i$.

299

ii) Case X>>1

For relatively large $\bar{X}_i$, $\mathrm{Tan}h(\bar{X}_i)\to 1$ according to Fig. 2 (a lower limit is $\bar{X}_i = 2$). Restricting analysis again on hydrograph shape parameters $m = 10$ (for all portions of a cascade), $Q_{max,i} = 0.69$ from Eqs. (10,11). Consequently, maximum lateral inflow to the small stream is

$$p_2^* \equiv \frac{0.69\, K_1 S_{0,1}^{1/2} p_1^{*\,5/3} t_1^{*\,5/3}}{b_1} = \frac{0.69\, p_1^* x_1}{b_1 X_1} \tag{25}$$

With $t_{max,1} = t_2^* = t_1^*(1.1+0.4\,X_1)$ according to Eq. (13) and p_2^* from Eq. (25)

$$X_2 = \frac{\chi X_1^{5/3}}{(0.69)^{2/3}(1.1+0.4X_1)^{5/3}} \tag{26}$$

and

$$q_{max,2} = K_2 S_{0,2}^{1/2} p_2^{*\,5/3} t_2^{*\,5/3} Q_{max,2} = \frac{0.69\, p_2^* x_2}{X_2} \tag{27}$$

whence, with Eqs. (25) and (26)

$$q_{max,2} \equiv \frac{0.69^{8/3}(1.1+0.4X_1)^{5/3}}{\chi X_1^{8/3}} \frac{p_1^* x_1 x_2}{b_1} \tag{28}$$

Non-dimensional maximum discharge per unit width at the watershed outlet may be expressed as

$$\hat{q} = \frac{q_{max,2}\, b_1}{p_1^* x_1 x_2} \tag{29}$$

thus

$$\hat{q}(X_i \gg 1) = \frac{0.69^{8/3}(1.1+0.4X_1)^{5/3}}{\chi X_1^{8/3}} \tag{30}$$

In contrast to case i), in which $\hat{q} = 1$ from Eq. (16), case ii) depends on both, χ and X_1. An asymptotic solution for $X_i\to\infty$ is

$$\hat{q}(X_i\to\infty) = \frac{0.081}{\chi X_1} \tag{31}$$

from Eq. (30) or, by redimensionalizing

$$q_{max,s} \equiv K_2 S_{0,2}^{1/2} \left(\frac{2x_1 t_1^* p_1^*}{9b_1} \right)^{5/3} \tag{32}$$

in which $2x_1 p_1^* t_2^*/(9b_1)$ is identified as maximum stream flow depth, $h_{max,s}$. Consequently, case ii) does not depend on the flow characteristics of the catchment area ($K_1 S_{0,1}^{1/2}$) nor on the stream length x_2.

Relative lengths X_i become *long* (say $X_i > 2$) provided

- x_i are long (considerable surface of catchment area, almost quadratic shape),
- p_i^* are small (small excess precipitation),
- t_i^* are short (times to peak are short, say some minutes).

Comparing these properties of case ii) with the basic requirements of the present hydrological model (heavy excess precipitation, relatively small catchment areas) it is noted that $X_i \gg 1$ must usually be excluded. Since X_i depends significantly on t_i^*, $X_i \propto t_i^{*-5/3}$, and having Eq. (13) in mind, it is unrealistic that $X_2 \gg 1$ if $X_1 \gg 1$.

iii) Case $0.3 \leqslant X_i \leqslant 2$

For intermediate values of X_i effects of cases i) and ii) appear simultaneously. Appendix II contains a complete derivation governing this case; the main results may be summarized as follows:

a) It is usefull to introduce the function

$$\phi_i(X_i) \equiv \frac{Tanh(X_i/0.69)}{X_i/0.69} \tag{33}$$

by which all needed relations for the hydrograph at the basin outlet may be represented.

b) Time to peak of the hydrograph at the watershed outlet becomes

$$\frac{t_{max,s}}{t_1^*} \equiv (1.1+0.4X_1)\left(1.1 + \frac{0.4\chi X_1}{\phi_1^{2/3}(1.1+0.4X_1)^{5/3}}\right) \tag{34}$$

which is plotted in Fig. 7. Note that $\chi \ll 1$ usually according to the statements in case i), whence $t_{max,s}/t_1^*$ may approximately be determined by Eq. (22), for which $\chi = 0$.

c) Maximum discharge per unit width at the basin outlet obtains

$$\hat{q} \equiv \phi_1(X_1)\phi_2(X_2) \tag{35}$$

in which $\hat{q}$ is defined in Eq. (29). This is plotted in Fig. 8 as $\hat{q} = \hat{q}(X_1, \chi)$. Note that $\hat{q}(X_i \ll 1) \rightarrow 1$ (case i)), while $\hat{q}(X_i \gg 1)$ (case ii)) is given by Eq. (30).
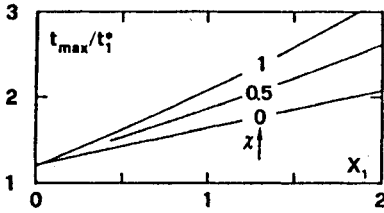
301

Fig. 7. Relative time to peak $t_{max,s}/t_1^*$ at the basin outlet as a function of X_1 for various typical χ accoring to Eq. (21).

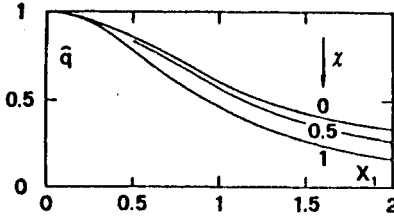

Fig. 8. Relative maximum discharge, $\hat{q}$, according to Eq. (29) at the basin outlet in function of X_1 for various typical χ according to Eq. (21).

Computational Procedure

The computational procedure may be summarized as follows:

1) Basic Parameters

Catchment area roughness coefficient K_c, average bottom slope $S_{0,c}$, lengths $x_{c,1}$ and $x_{c,2}$ (two sided);

Small stream roughness coefficient K_s, average bottom slope $S_{0,s}$, length x_s and stream width B, whence $b_1 = (x_{c,1}/(x_{c,1}+x_{c,2}))B$;

Precipitation excess rainfall characterized by P_c^* and t_c^* so that $m = 10$ (the peak zone of the excess hyetograph should be particularly well modelled).

2) Non-Dimensional Length X_c

The non-dimensional length of one of the sides of the catchment area (usually the longer one) is given by Eq. $(5)_2$

$$X_1 = X_c = \frac{x_{c,1}}{K_c S_{0,c}^{1/2} P_c^{*2/3} t_c^{*5/3}} \tag{36}$$

in which all coefficients are given in 1).

3) Runoff Number χ

Apart from X_1, runoff is characterized by the runoff number χ given in Eq. (21)

$$\chi = \frac{x_s}{x_{c,1}} \left(\frac{b_1}{x_{c,1}} \right)^{2/3} \left(\frac{K_c S_{0,c}^{1/2}}{K_s S_{0,s}^{1/2}} \right) \tag{37}$$

302

This number will usually be small.

4) Application of Diagrams

Runoff process over catchment area and along the small stream is analysed using Figs. 7 and 8, the result being the hydrograph at the watershed outlet. The plots yield $t_{max,s}$ and $q_{max,s}$ in terms of $X_c (= X_1)$ and χ. Introducing the parameters

$$\hat{T} \equiv \frac{t}{t_{max,s}} \qquad \hat{Q} \equiv \frac{q}{q_{max,s}} \qquad (38)$$

then finally allows the hydrograph to be expressed as

$$\hat{Q}(\hat{T}) = [\hat{T} \exp(1-\hat{T})]^{10} \qquad (39)$$

Maximum discharge at the watershed outlet becomes $\bar{Q}_{max,s} = q_{max,s}B$ in $(m^3 s^{-1})$.

5) Model Verifications

The kinematic wave approximation holds only if

i) dynamical waves are damped and flow conditions are globally subcritical, corresponding to $\mathbf{F} < 1$ or, according to Appendix I

$$(K\sqrt{S_0})_i < 3 \qquad (40)$$

$\mathbf{F}_{max,i}$ is the maximum Froude number of flow at the lateral stream inflow and at the basin outlet, and K $(m^{1/3}/s) = 1/n$ is Manning's roughness coefficient.

ii) the flow is very shallow, i.e. $[h/(S_0 \times x)]_{max,i} \ll 1$ or, according to Hager and Hager (1985)

$$p_{max,i} < \frac{0.07 \, g^2}{(K^3 \sqrt{S_0})_i} \qquad (41)$$

The numbers at the right hand side of Eqs. (40) and (41) should be regarded as informational indications.

Example

Consider a symmetrical catchment area with $x_{c,1} = x_{c,2} = 1,500$ m and a small stream of length $x_s = 6,000$ m along its center. Average bottom slopes are $S_{0,c} = 0.1$ and $S_{0,s} = 0.02$, respectively, and roughness coefficients according to Manning's formula may be estimated as $K_c = 10 \; m^{1/3}s^{-1}$ and $K_s = 20 \; m^{1/3}s^{-1}$. The excess hyetograph can be approximated by $p_c^* = 20$ mm/h, $t_c^* = 1.5$ h and $m_c = 10$. Find the resulting hydrograph at the watershed outlet for a stream width $B = 10$ m.
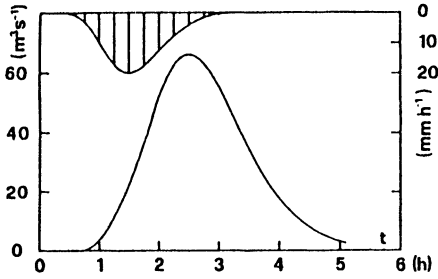
Fig. 9. Hyetograph $p \equiv p(t)$ according to example with $p_1^* \equiv 20$ mm/h and resulting hydrograph $\tilde{Q} \equiv \tilde{Q}(t)$ at the watershed outlet.

1) Basic parameters: $K_c = 10$ m$^{1/3}$s^{-1}, $S_{0,c} = 0.1$, $x_c = 1,500$ m,
$K_s = 20$ m$^{1/3}$s^{-1}, $S_{0,s} = 0.02$, $x_s = 6,000$ m,
$P_c^* = 5.6{\times}10^{-6}$ ms^{-1}, $t_c^* = 5,400$ s, $m_c = 10$.

2) Non-dimensional length X_c: Inserting these values in Eq. (36) results in
$$X_c = X_1 = 0.91.$$

3) Runoff number: With $b_1 = B/2$ and Eq. (37) the runoff number is $\chi = 0.10$.

4) Application of diagrams: Fig. 7 yields $t_{max,s}/t_c^* = 1.65$, thus $t_{max,s} \simeq 2.5$ h; Fig. 8 gives $\hat{q} = 0.66$, thus $q_{max,s} = 5.6{\times}10^{-6}$ $1,500{\times}6,000 \times 0.66/5$ $= 6.6$ m^{2}s^{-1} and finally $\tilde{Q} = q_{max,s} B = 66$ m^{3}s^{-1}.

Accounting for the scalings in Eq. (38) allows determination of the hydrograph at the watershed outlet (see Fig. 9). Also included in the plot is the governing excess hyetograph, and it is noted that the time difference between the two maxima is $\Delta t = 1$ h.

5) Dynamical wave condition, $(K\sqrt{S_0})_c = 3.1$ and $(K\sqrt{S_0})_s = 2.8$ is near the limit but fulfilled. The diffusive wave condition Eq. (41), $p_{max,c} = 5.6{\times}10^{-6}$ ms$^{-1} <$ 0.021 ms^{-1} and $p_{max,s} = q_{max,s}/X_s = 6.6/6,000 = 1.1{\times}10^{-3}$ ms$^{-1} < 6{\times}10^{-3}$ ms^{-1} are also satisfied.

As a consequence the solutions according to the kinematic wave approximation and the de Saint Venant flow equations are nearly identical.

Conclusions

The present investigation examines non-linear runoff process resulting of time-dependent excess precipitation by means of the kinematic wave theory. Considerations include a watershed consisting of two rectangular planes (catchment area) and a small stream situated at its downstream zone. Explicit solutions are given for the hydrograph at the watershed outlet. The following conclusions are immediate:

1) Solutions of a recent investigation concerning runoff from a singular cascade can be approximated in terms of the original input function (excess rainfall). The resulting main features of the hydrograph, namely maximum discharge and corresponding time to peak, and the hydrograph shape parameter are specified for arbitrary geometrical and hydrological parameters.

2) A discussion of particular cases with respect to the non-dimensional length X reveals a simple (and realistic) case for small X. Maximum discharge at the basin outlet is then equal to maximum excess precipitation times the surface of the catchment area. This result holds for both steady and non-steady flow conditions (with a single-peaked hyetograph). Further, it is shown that large X violate the assumptions governing the present hydrological rainfall runoff model.

3) Finally, intermediate values of X are considered and plots enable a direct and rapid determination of the resulting hydrograph at the watershed outlet. Criteria concerning the applicability of the kinematic wave approach are given.

4) maximum discharge at the watershed outlet depends on the non-dimensional catchment area length X_c and the runoff number χ specified in Eq. (21). χ accounts for the geometrical properties of the catchment area and the small stream.

5) The computational procedure for the cascade »catchment area-small stream« is discussed and illustrated by examples. All pertinent relations for the sought hydrograph are given analytically; analysis is straightforward once the basic parameters are specified. This particular feature of the present hydrological rainfall-runoff model allows a simple prediction of hydrographs in small watersheds under heavy excess precipitation.

Notations

Some of the notations appear with indices *"c"* and *"s"* and refer then to catchment area and small stream, respectively; accordingly, indices "1" and "2", ... refer to the first, second, and following hydrological cascades. * denote maxima of lateral inflow, while "max" refer to the maxima of the resulting cascade outflow. Index "abs" refers to the maximum possible discharge.

b	[m]	portion of stream width relating to one side of the catchment area
B	[m]	total stream width as an average
F	[-]	Froude number
g	[ms^{-2}]	gravitational acceleration
h	[m]	flow depth
K	[m$^{1/3}$s^{-1}]	roughness coefficient according to Strickler's formula
m	[-]	hydrograph shape parameter

305

n	$[m^{-1/3}s^1]$	roughness coefficient according to Manning's formula
p	$[ms^{-1}]$	excess precipitation
q	$[m^2s^{-1}]$	discharge per unit width
$\hat{q}$	$[-]$	relative maximum discharge per unit width according to Eq. (29).
Q	$[-]$	non-dimensional discharge according to Eq. (5)
$\bar{Q}$	$[m^3s^{-1}]$	discharge
$\bar{Q}$	$[-]$	non-dimensional discharge according to Eq. (9)
S_0	$[-]$	average bottom slope
S_f	$[-]$	friction slope
t	$[s]$	time
T	$[-]$	non-dimensional time according to Eq. (5)
$\bar{T}$	$[-]$	non-dimensional time according to Eq. (12)
x	$[m]$	longitudinal coordinate
X	$[-]$	non-dimensional longitudinal coordinate according to Eq. (5)
$\bar{X}$	$[-]$	non-dimensional longitudinal coordinate according to Eq. (9)
Y	$[-]$	non-dimensional flow depth according to Eq. (5)
χ	$[-]$	runoff number according to Eq. (21)
ψ	$[-]$	diffusion number
ϕ	$[-]$	auxiliary function

References

Eagleson, P. S. (1970). *Dynamic Hydrology,* McGraw Hill Book Company, New York.

Hager, W. H. (1984a). A simplified hydrological rainfall-runoff model, *J. Hydrology, Vol. 74,* pp. 151-170.

Hager, W. H. (1984b). Effects of local bottom slope and roughness coefficient variations in overland flow, *Nordic Hydrology, Vol. 15,* pp. 131-144.

Hager, W. H., and Hager. K. (1985). Application limits for the kinematic wave approximation, *Nordic Hydrology, Vol. 16*, pp. 203-212.

Jason, J.-F. (1982). Contribution à l'étude des relations pluies-débits dans les petits bassins versants ruraux, Thèse No 43, presented at the Swiss Federal Institute of Technology of Lausanne, EPFL, Switzerland, for the requirements of Doctor of Sciences, Lausanne.

Lighthill, M. H., and Whitham, G. B. (1955). On kinematic waves, part I, *Proc. Roy. Soc. A, Vol. 229,* pp. 281-316.

Raudkivi, A. J. (1979). *Hydrology,* Pergamon Press, Oxford-New York.

Sinniger, R., and Hager, W. H. (1984). Retentionsvorgänge in Speicherseen, (Storage effects in reservoirs), *Schweizer Ingenieur und Architekt, Vol. 102,* pp. 535-539.

Wooding, R. A. (1965, 1966) A hydraulic model for the catchment stream problem, *J. Hydrology, Vol. 3,* pp. 254-282; *Vol. 4,* pp. 21-37.

Appendix I *Conditions i), ii) and the kinematic wave approach*

Kinematic wave theory requires that i) Froude numbers be always smaller then unity and ii) maximum flow depth be much smaller than the difference of elevations of a typical reach. Maximum Froude number may be defined as

$$\mathbb{F}_{max} = \left(\frac{q}{\sqrt{gh^3}}\right)_{max} \tag{42}$$

in which index "max" relates to both, q and h. According to Eq. (16) $q_{max,s} = p_1^* x_1 x_2 / b_1$, and the relation between flow depth and discharge per unit width is given by Eqs. (2) and (3)

$$h \equiv \left(\frac{q}{KS_0^{1/2}}\right)^{3/5} \tag{43}$$

Inserting this into Eq. (42) results in

$$\mathbb{F}_{max} \equiv q_{max}^{1/10} \, K^{9/10} \, S_0^{9/20} \, g^{-1/2} \tag{44}$$

Since the order of maximum discharge per unit width in small streams will be approximately $0.1 \leqslant q_{max} \leqslant 10 \text{ m}^2\text{s}^{-1}$, its effect on $\mathbf{F}_{max}$ is insignificant, $\mathbf{F}_{max}(q_{max}) \propto 0$ (1). With $g^{-1/2} = 0.32 \text{ m}^{-1/2}\text{s}$, the necessary condition for both catchment area and small stream is

$$(K\sqrt{S_0})_i < 3 \tag{45}$$

in which K ($\text{m}^{1/3}\text{s}^{-1}$) and S_0 (-). Dynamical effects of wave propagation, therefore, are absent for flows over *rough, slightly sloped surfaces*.

Condition ii) requires

$$\psi \equiv \frac{h_{max,i}}{S_{0,i} x_i} \ll 1 \tag{46}$$

This criterion cannot be further simplified from this point of view. However, detailed investigation into the kinematic wave pattern allows definition of $\psi = (pK^3\sqrt{S_0}/g^2)_{max,i} < 0.07$ (Hager and Hager 1985).

Appendix II *Hydrographs at the watershed outlet for intermediate values of X_i*

Maximum discharge is given by Eq. (11) or by Eq. (14) for m = 10, whence, upon inserting $\phi_i(X_i)$ according to Eq. (33)

$$Q_{max,i} = X_i \frac{T \text{anh}(X_i/0.69)}{X_i/0.69} = X_i \, \phi_i(X_i) \tag{47}$$

in which $0 \leqslant \phi_i \leqslant 1$. For given X_1, one determines for $Q_{max,2} = X_2\phi_1$, whence

307

$$p_2^* = \frac{q_{max,1}}{b_1} = \frac{x_1 p_1^* \phi_1}{b_1} \tag{48}$$

Further, with $t_2^* = t_1^* (1.1+0.4X_1)$ and

$$X_2 = \frac{x_2}{K_2 S_{0,2} p_2^{*2/3} t_2^{*5/3}} = \frac{\chi X_1}{\phi_1^{2/3} (1.1+0.4X_1)^{5/3}} \tag{49}$$

and with Eq. (18)

$$\frac{t_{max,s}}{t_1^*} = (1.1+0.4X_1)(1.1+0.4X_2) =$$

$$= (1.1+0.4X_1)(1.1 + \frac{0.4\chi X_1}{\phi_1^{2/3} (1.1+0.4X_1)^{5/3}}) \tag{50}$$

This depends only on X_1 and χ and is plotted in Fig. 7 for $0 \leqslant X_1 \leqslant 2$ and typical values of χ. With Eq. (47) maximum discharge of cascade "2" obtains

$$Q_{max,2} = X_2 \phi_2 \tag{51}$$

in which X_2 is given by Eq. (49) such that

$$q_{max,2} = K_2 S_{0,2}^{1/2} p_2^{*5/3} t_2^{*5/3} Q_{max,2} \tag{52}$$

$$q_{max,2} = x_2 p_2^* \phi_2 \tag{53}$$

Inserting Eq. (48) then yields

$$q_{max,2} \equiv \frac{x_1 x_2 p_1^*}{b_1} \phi_1(X_1) \phi_2(X_2) \tag{54}$$

so that finally

$$\hat{q} = \phi_1(X_1) \phi_2(X_2) \tag{55}$$

according to Eq. (21). Using Eq. (49) to express X_2 in terms of X_1 and χ, $\hat{q} = \hat{q}(X_1, \chi)$; the result is plotted in Fig. 8.

Address:
École Polytechnique Fédérale de Lausanne,
Département de Génie Civil,
Institut de Travaux hydrauliques, CCH,
CH-1015 Lausanne, Switzerland.